Enhancement of Tubular Cross-Flow Microfiltration of Dispersions by Gas-Liquid Two-Phase Flow*

P. POSPÍŠIL, P. MIKULÁŠEK**, P. DOLEČEK, and J. CAKL

Department of Chemical Engineering, University of Pardubice,
CZ-532 10 Pardubice
e-mail: Petr.Mikulasek@upce.cz

Received 4 April 2001

An application of the gas-liquid two-phase flow for the flux enhancement during the microfiltration of aqueous titanium dioxide dispersions on aluminium oxide tubular membrane has been studied. This study focused on the influence of the liquid and gas flow velocities and feed concentration on the flux and on the development of a mathematical model for the flux prediction. The results of experiments showed a positive effect of the constant gas-liquid two-phase flow on the flux. It might be concluded from the analysis of experimental results based on dead-end filtration model that two-phase flow seemed to expand the particle cake as it increased both the cake porosity and thickness, thus allowing higher fluxes. For the periodical gas flow, the flux enhancement was not so significant and strongly depended on the periodical gas flow mode as well as on the concentration of dispersion used. On the other hand, an air injection influenced the permeate flux for any concentration studied. A mathematical model for the flux prediction during the two-phase gas-liquid microfiltration has been developed. The results showed a good agreement between experimental data and model prediction.

A rapid permeate flux decrease at the beginning of the filtration is the general problem of the cross-flow microfiltration and ultrafiltration. The deposition of particles on the membrane surface and inside pores makes microfiltration ineffective since it diminishes the flux and increases the energy consumption for required separation. The steady-state permeate flux may be as low as 2—10 % of that of pure water flux. Therefore, there is a tremendous potential to reduce or control concentration polarization and fouling in membrane processes and hence alleviate these limitations. Many techniques for reduction of particle deposition and concentration polarization have been studied. Still, some of them have not been experimentally tested yet. The survey of these methods is summarized in [1]. There are at least three possible approaches to reduce or control the concentration polarization and fouling: changes in surface characteristics of the membrane; pretreatment of the feed; and fluid management methods.

Recently, some studies have referred to the area of use of gas-liquid two-phase flow techniques in the concentrate stream during ultrafiltration in order to enhance the flux for different applications (biological treatment, drinking water production, macromolecules separation) and different membrane geometries (hollow fibre, flat sheet or tubular). The application of gas-liquid two-phase flow for microfiltration and ultrafiltration intensification is based on a change of hydrodynamic conditions inside the membrane module, which positively increases the wall shear stress, thus preventing the membrane fouling and enhancing the mass transfer of the separated compound (solvent, most frequently water).

At present, studies of two-phase gas-liquid flow in membrane filtration processes have mostly experimental character and are goal-directed on ultrafiltration. Only very few research works have been focused on the theoretical aspects of the process. *Cui et al.* [2—4] have shown that air injection can reduce the concentration polarization in ultrafiltration of macromolecules (dextran, dyed dextran, and bovine serum albumin) in the case of flat sheet modules and hollow fibre membranes. The explanation given for the flux enhancement is that air sparging into the liquid stream increases turbulence near the membrane surface as well as the cross-flow velocity, thus limiting the boundary layer thickness. *Mercier et al.* [5, 6] reported a significant flux enhancement (200 % of flux increase) by air sparging in ultrafiltration tubular in-

*Presented at the 28th International Conference of the Slovak Society of Chemical Engineering, Tatranské Matliare, 21—25 May 2001.

**The author to whom the correspondence should be addressed.

organic membranes with two kinds of suspension (bentonite and yeast).

Cabassud et al. [7, 8] have presented results concerning two-phase gas-liquid flow for particle suspensions (clay suspensions) inside hollow fibres. In these cases, flux improvement was linked to the hydrodynamic control of the particle deposition on the membrane. For all studied concentrations, significant increases in permeate flux have been observed even at a very low air velocity. The air injection process leads to an increase of up to 155 % at specific conditions. However, good results have been obtained for very low air velocities (under 0.2 m s^{-1}). *Lee et al.* [9] used air slugs entrapped in cross-flow stream to prevent the flux decline during filtration of bacterial cell suspensions. Ultrafiltration and microfiltration flat sheet membranes have been used and the best performance was obtained for the ultrafiltration (maximum enhancement of 200 % is reported).

An accurate model that would enable to predict the permeate flux during microfiltration with two-phase flow has not been proposed yet. *Vera et al.* [10] expressed a steady-state flux of gas-sparged microfiltration and ultrafiltration using two dimensionless numbers: generalized shear stress number and resistance number. The validations of graphic relations between them and explanation of the line slopes have to be confirmed by another experiments. Experiments of *Vera et al.* [10] were carried out with dextran, wastewater effluent, tap water, and ferric hydroxide suspensions. The maximum flux enhancement of 200 % was achieved. The ultrafiltration model of *Ghosh* and *Cui* [11] was based on a diffusion mechanism of permeate transport through the membrane surface and gave predicted flux values lower than experimental ones. The model consisted in dividing the two-phase flow in membrane into three zones enclosed in one gas slug.

The aim of this study is to explain the influence of two-phase gas-liquid flow on the flux, determine which operating parameters are involved in the flux enhancement, and propose a semi-empirical model for the time-dependent flux prediction. Such model assumes that a nondiffusive transport phenomenon is the main mechanism of particles back-transport from a membrane surface and thus the diffusion can be neglected. The validation of this model by laboratory experiments is also presented.

THEORETICAL

Cakl et al. [12] developed a semi-empirical model describing the time-dependent decrease of permeate flux modified for backflushed cross-flow microfiltration. Their model was derived from a dead-end filtration model in which cake resistance was determined by the mass accumulated during the time of initial flux decrease. This procedure has been shown to yield a very good approximation to the exact solution for a time-variable permeate flux, J [13].

The particle mass balance adapted for the backflush [12] is given by

$$\left[(J - J_{\mathrm{S}}) + \frac{\mathrm{d}\delta_{\mathrm{C}}}{\mathrm{d}t}\right] \Phi_{\mathrm{F}} = \Phi_{\mathrm{C}} \frac{\mathrm{d}\delta_{\mathrm{C}}}{\mathrm{d}t} \qquad (1)$$

where J is the permeate flux, J_{S} the steady-state flux without backflushing, Φ_{F}, Φ_{C} are the solid volume fractions in the suspension and in cake, respectively, and δ_{C} is the cake layer thickness. The product $J_{\mathrm{S}}\Phi_{\mathrm{F}}$ is suggested to describe the particle flux out of the membrane wall. This model has been experimentally proved for the backflush microfiltration of various suspensions and emulsions [12].

Considering that the transport of particles from the membrane wall is proportional to the velocity gradient on the membrane surface in the case of gas-liquid microfiltration, the influence of gas flow velocity should be represented in the particle mass balance. Then, the particle mass balance for the microfiltration with gas-liquid two-phase flow is expressed by

$$\left[(kJ - J_{\mathrm{S}}) + \frac{\mathrm{d}\delta_{\mathrm{C}}}{\mathrm{d}t}\right] \Phi_{\mathrm{F}} = \Phi_{\mathrm{C}} \frac{\mathrm{d}\delta_{\mathrm{C}}}{\mathrm{d}t} \qquad (2)$$

where J_{S} is the steady-state flux during microfiltration without two-phase flow. The quantity k indicates the influence of gas sparging on the immediate permeate flux.

The resistance model is expressed by

$$J = \frac{\Delta P}{\eta_0 R_{\mathrm{T}}} \qquad (3)$$

where ΔP is the transmembrane pressure, η_0 the dynamic viscosity of the permeate, and R_{T} the total resistance to permeate flow, which can be defined as

$$R_{\mathrm{T}} = R_{\mathrm{M}} + R_{\mathrm{R}} + R_{\mathrm{IR}} \qquad (4)$$

where R_{M}, R_{R}, and R_{IR} are the membrane, reversible, and irreversible resistances, respectively. The irreversible resistance represents the membrane pores blocking due to the particle size or adsorption phenomena. When the particles cannot enter into the membrane pores, *e.g.* when a large gap between the biggest pore diameter and the smallest particle diameter exists, the irreversible resistance can be neglected. The reversible resistance is actually the cake resistance (thereinafter called R_{C}), which could be expressed as a product of specific cake resistance (R'_{C}) and cake thickness. According to the Darcy's equation, the flux is defined as

$$J = \frac{\Delta P}{\eta_0(\delta_{\mathrm{C}} R'_{\mathrm{C}} + R_{\mathrm{M}})} \qquad (5)$$

Combining eqns (*2*) and (*5*) the following differential equation is obtained

$$-\frac{1}{J^2}\frac{1}{(kJ-J_\mathrm{S})}\mathrm{d}J=\frac{\Phi_\mathrm{F}\eta_0 R'_\mathrm{C}}{(\Phi_\mathrm{C}-\Phi_\mathrm{F})\,\Delta P}\mathrm{d}t \qquad (6)$$

For the integration of eqn (*6*), the following conditions are considered: the initial flux is equal to the pure water permeate flux ($J=J_0$; $t=0$); the specific cake resistance is constant over the period of filtration; and the filtration cake is incompressible.

The following expression for the time-dependent permeate flux is a result of the integration

$$J=\left[\frac{1}{J_0}+\frac{k}{J_\mathrm{S}}\ln\left(\frac{kJ_0-J_\mathrm{S}}{kJ-J_\mathrm{S}}\frac{J}{J_0}\right)-\frac{J_\mathrm{S}\Phi_\mathrm{F}\eta_0 R'_\mathrm{C}}{(\Phi_\mathrm{C}-\Phi_\mathrm{F})\,\Delta P}t\right]^{-1} \qquad (7)$$

where J_0 is the pure water permeate flux, J_S the steady-state flux during microfiltration without two-phase flow, t time, and η_0 the dynamic viscosity of the permeate. Two experimental measurements have to be done before the calculation. First, with pure water for J_0 and R_M evaluation, and then a microfiltration experiment without two-phase flow to obtain the values of J_S and specific cake resistance calculated from dead-end filtration model ($R'_\mathrm{C,D\text{-}E}$) [14]. The value of Φ_C was substituted by the maximum solid volume fraction in filtration cake (0.65), reported in [14]. The gas flow, k, as an exponential function of injecting factor, r, was estimated from previous measurements [15]

$$k=\exp(-r) \qquad (8)$$

The injecting factor, r, is defined as

$$r=\frac{u'_\mathrm{G}}{u'_\mathrm{G}+u'_\mathrm{L}} \qquad (9)$$

where u'_G and u'_L are superficial gas and liquid flow velocities, respectively.

The expression of specific cake resistance during the microfiltration with two-phase flow is based on the specific cake resistance during the microfiltration without two-phase flow ($R'_\mathrm{C,D\text{-}E}$). The relation between R'_C and $R'_\mathrm{C,D\text{-}E}$ is a function of k valid for the whole gas flow velocity range

$$R'_\mathrm{C}=kR'_\mathrm{C,D\text{-}E} \qquad (10)$$

Then, the flux, J, for various gas flow velocities during the microfiltration with two-phase flow could be predicted. Eqn (*7*) is implicit in J and can be solved, *e.g.* in MS Excel with program Solver.

EXPERIMENTAL

The microfiltration experiments were performed with an aqueous dispersion of titanium dioxide (Versanyl B-K7020) obtained from Ostacolor a.s., Pardubice, Czech Republic. The mean diameter of particles was 443 nm, however, the distribution of particle size was very wide (from 210 nm to 850 nm). The solids content in the dispersion was 1 mass % and 5 mass % during the microfiltration experiments. During concentration experiments, the dispersion solids content increased from 5 mass % to 18 mass %. The dispersion of titanium dioxide was stable during the experiments.

The membranes used in the experiments with two-phase gas-liquid flow were asymmetric multi-layered ceramic membranes (Terronic a.s., Hradec Králové, Czech Republic). Composed of a thin alumina layer deposited on the internal surface of the alumina support, the membranes were configured as single 0.1 m long, 6 mm i.d., and 10 mm o.d. cylindrical tubes. The microfiltration membranes with the 91 nm mean pore diameter were used in microfiltration experiments. The pore size distribution of the membrane was determined by the liquid displacement method [16].

The two-phase gas-liquid apparatus used in our experiments was shown schematically in [14]. The stainless steel circulating loop contained a 5 dm^3 retentate tank, a diaphragm pump, a membrane module, and a flow control valve at the module outlet. The loop was also equipped with a thermal regulating system, and pressure, temperature, and flow monitoring systems. The velocity and pressure in the retentate loop were varied independently by means of a pump controller and an appropriate needle valve. Air was added to the liquid stream through a capillary at the inlet of the membrane. The airflow rates were controlled by means of a flowmeter.

After the membrane had been placed in the membrane module, distilled water was circulated in the test loop at the moderate operating pressure for about 2 h. During this time a stabilization of the membrane was observed giving relatively stable water permeability. Then, a feed substance concentrate preheated to a desired temperature (25 °C) was introduced to the unit and the operating pressures as well as the retentate velocity were adjusted by the regulation system.

The flux through a membrane was measured by weighing the permeate collected during a chosen period of system operation (using a computer-interfaced balance). Both, the retentate and permeate were recirculated back into the retentate container. Therefore, the concentration in the recirculation loop remained virtually constant. After each set of experiments was finished, the circuit and membrane were rinsed with water and the pure water flux was measured again under the conditions of initial testing until the steady state was obtained. The differences of subsequent steady-state pure-water fluxes were

taken as a measure of the membrane fouling tendency.

RESULTS AND DISCUSSION

Constant Gas Flow

The direct observations of two-phase gas-liquid flow mode through the transparent tubular pipe (of the same i.d. as the membranes) confirmed the published results [17]. Each flow pattern corresponded to the value of superficial gas velocity, u'_G, and the superficial liquid velocity, u'_L, respectively. Both values were calculated as if each phase was circulating separately. For a given liquid velocity, the main structures observed when the gas velocity was increased, included the bubble flow, slug flow, churn flow, and annular flow. Previous studies showed that slug flow is the most efficient regime giving significant enhancement of the mass transfer [5, 7]. Moreover, for a given liquid flow rate, the presence of gas increases the mean longitudinal velocity of the fluid, and in association with the great variations in the wall shear stress and the turbulence, it can improve the process performance.

The effects of gas-liquid two-phase flow on permeate flux were measured at various experimental conditions keeping constant the liquid flow velocity 1 m s^{-1} and transmembrane pressure difference 100 kPa. The permeate flux obtained in the presence of gas was always larger than that without gas flow. Fig. 1 shows the results of experiments realized with and without two-phase flow in the feed stream. A typical behaviour

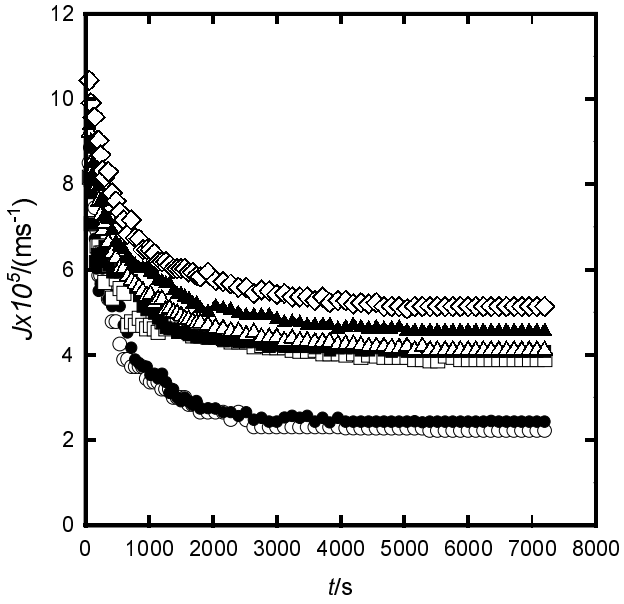

Fig. 1. Influence of a constant gas-liquid flow on immediate permeate flux for $u'_L = 1$ m s^{-1}, $\Delta P = 100$ kPa, $w_F = 0.01$, and gas injecting capillary i.d. 1.08 mm. u'_G/(m s^{-1}): ○ 0, ● 0.25, □ 0.53, ■ 0.81, △ 1.11, ▲ 1.70, ◇ 2.36.

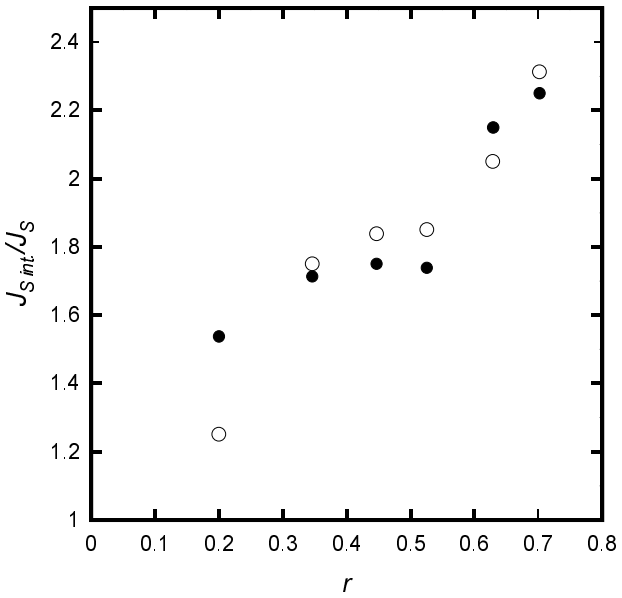

Fig. 2. Normalized steady-state permeate flux against injecting ratio for 1.08 mm (○) and 2.31 mm (●) i.d. capillaries ($u'_L = 1$ m s^{-1}, $\Delta P = 100$ kPa, $w_F = 0.01$).

for cross-flow microfiltration when the permeate flux without injecting air in the feed stream decreases with time, was observed. During the first few minutes the flux decreased sharply, due to a particle deposit formation that constituted an additional flow resistance. Then the flux seemed to level off. The deposit behaved like a second membrane, with a constant flow resistance with time.

In the experiments using two-phase flow, air was injected throughout the filtering period. Here an initial flux decline was also observed but it was less important than the one observed without air injection. When the gas velocity was higher, the flux was maintained at a higher level during the filtering period as shown in Fig. 1. The values of the normalized steady-state permeate flux are plotted as a function of injecting ratio, r, in Fig. 2. The normalized permeate flux first increased with the air velocity until it reached a limit corresponding to $u'_G = 0.8$ m s^{-1}. That is to say that a further increase in air velocity would not result in any significant improvement in the permeate flux until the change of flow conditions. For $u_G = 0.5$—1.25 m s^{-1}, large bubbles were observed with size of the order of the internal diameter of the tube (Taylor bubbles). Due to reduction in the available cross-section for the liquid phase, a thin liquid film always remained over the surface of the membrane and moved in the opposite direction with respect to the main flow. This phenomenon induces a highly variable large shear rate against the pipe wall. It should be noted that for a given liquid flow rate, the presence of the gas increases the mean longitudinal velocity of the fluid which, in association with the great variations in the wall shear stress and the turbulence ex-

isting in the churn flow (u_G = 1.5—2.3 m s^{-1}), can improve the performance.

It is clear that increasing either liquid velocity or gas velocity will enhance permeate flux. However, the increase of liquid velocity will require more pump power than the increase of gas velocity. Accordingly, the same permeate flux obtained with a higher liquid velocity but without gas slugs can also be achieved with a lower liquid velocity and moderate gas velocity with gas slugs (u_G = 0.8 m s^{-1}), leading to the reduction of energy consumption. Moreover, it is interesting to notice that even at a relatively low velocity, the two-phase flow could enhance the flux (increase of 70 % for r = 0.35).

Periodical Gas Flow

Fig. 3 represents the evolution of the permeate flux *vs.* time for u'_G = 0 m s^{-1}, and for u'_G = 0.8 m s^{-1} for a constant and a periodical gas flow mode. In the periodical gas flow mode, a 10 min period of air flow alternated with a 30 min period without air injection. The permeate flux increased after 1.5 h in comparison with the flux without air for the feed content of 1 mass %. However, after each air flow interruption, the permeate flux decreased sharply. It can be better seen for the feed content of 5 mass % (see Fig. 3). Within the first minutes of air flow interruption, a particle deposit was created on the membrane surface, which was difficult to remove when the air injection was restored. The difference between the two modes is as follows: constant gas flow permits to prevent a cake deposit, whereas in the periodical gas flow air has to eliminate the deposit built up during the air flow interruption. At similar experimental operating conditions, a constant injection process is more efficient than a periodical one, for which higher air velocities may be necessary to sweep the deposit.

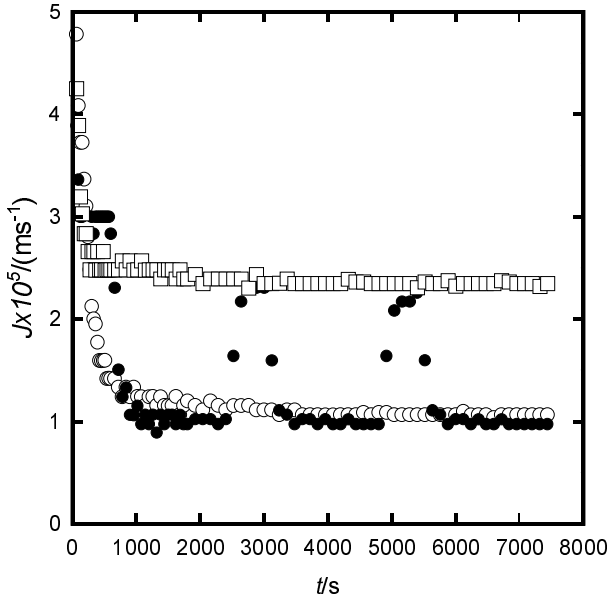

Fig. 3. Permeate flux for microfiltration without air addition (○), and with constant (□) or periodical (●) air flow for u'_L = 1 m s^{-1}, u'_G = 0.8 m s^{-1}, ΔP = 100 kPa, and w_F = 0.05. Periodical mode: 10 min with air flow, 30 min without air flow.

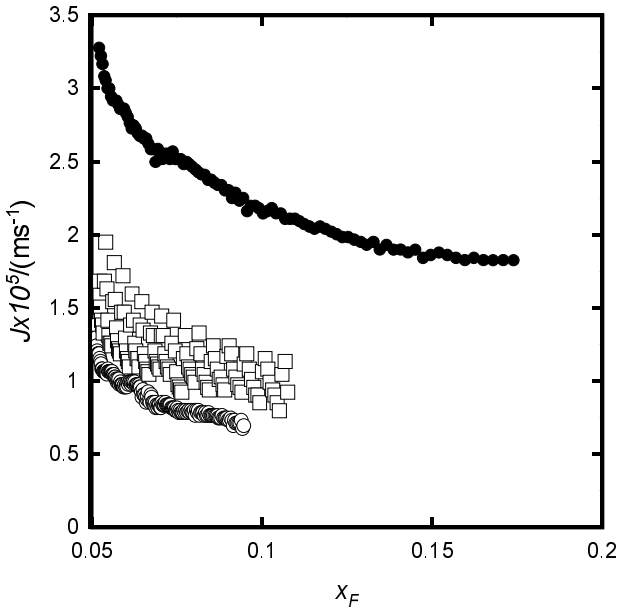

Fig. 4. Permeate flux *vs.* feed concentration for u'_L = 1 m s^{-1}, u'_G = 0.8 m s^{-1}, and ΔP = 100 kPa. Microfiltration without (○) and with constant (●), or periodical (□) air addition.

Effect of Particle Concentration

A study of the dispersion concentration effect on the permeate flux was undertaken by comparing the conventional single-phase cross-flow microfiltration to the two-phase flow membrane system in continuous or periodical air flow modes. Fig. 4 represents the relationship between the solid mass fraction of the dispersion and the permeate flux for the three modes tested. For u'_G = 0, the flux decreased sharply with concentration. This decrease may be related to the cake layer behaviour when the particle deposit became denser and less permeable. It is worthwhile that, compared to the filtration mode without intensification, the two-phase gas-liquid flow enabled processing of dispersion with twice higher solids concentration at the same filtration time.

Model Validation

A typical plot of flux *vs.* time showing a comparison of experimental results and the model prediction is shown in Fig. 5. The model developed in this study was able to describe the experimental filtration behaviour. However, an overestimation of the initial flux could be observed. Still, the prediction of the steady-

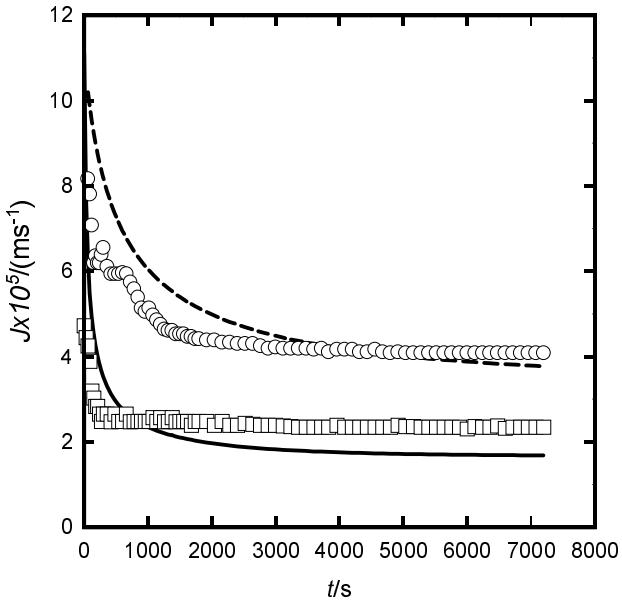

Fig. 5. Comparison of experimental fluxes with model prediction for $u'_{\mathrm{L}} = 1$ m s^{-1}, $u'_{\mathrm{G}} = 0.8$ m s^{-1}, and $\Delta P = 100$ kPa and for $w_{\mathrm{F}} = 0.01$ (○ – experiment, dashed line – model) and $w_{\mathrm{F}} = 0.05$ (□ – experiment, solid line – model).

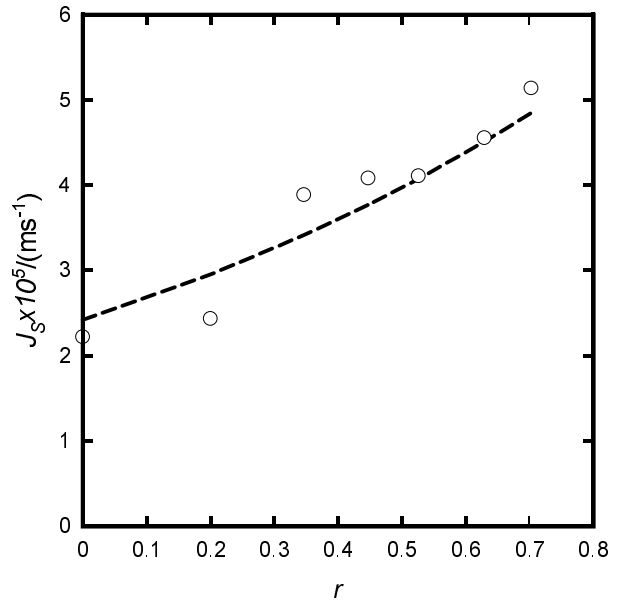

Fig. 6. Comparison of experimental (○) and predicted values (dashed line) of steady-state permeate flux for various injecting ratio and for $u'_{\mathrm{L}} = 1$ m s^{-1}, $\Delta P = 100$ kPa, $w_{\mathrm{F}} = 0.01$, and gas injecting capillary i.d. 1.08 mm.

state flux values is more important for industrial applications of two-phase gas-liquid flow in microfiltration processes.

Fig. 6 shows the values of steady-state permeate flux experimentally measured and predicted by the model. The values are predicted for the operation time of 2 h, when stable conditions for titanium dioxide dispersions filtration could be considered. The difference between experimental and model results varied from +20 % to −7 %. While for the low value of gas flow velocity ($r = 0.2$) the model overestimated the permeate flux, for higher gas flow velocities ($r = 0.3$—0.7) the model was nearly correct or slightly underestimated the fluxes. The overestimation in the range of $r = 0.1$—0.3 can be attributed to unstable flow conditions of bubble flow pattern observed.

CONCLUSION

The experimental results demonstrated that in cross-flow microfiltration of dispersions the gas-liquid two-phase flow is able to maintain the permeate flux at a constant and high level during the whole experimental run. The experiments carried out at a large number of flow conditions showed that periodical gas flow seems to be less effective than a constant one in similar experimental operating conditions. However, the permeate flux improvement for periodical mode was observed compared to experiments without an air addition. The intensification ability of the periodical gas flow depends on the periodical gas flow mode and on the dispersion concentration. The hydrodynamic regime inducing the largest enhancement in flux is slug flow in the case of aqueous titanium dispersion where a permeate flux plateau is reached at the beginning of the slug flow regime. Application of slug flow pattern is a good compromise between the flux enhancement and the air consumption during the microfiltration process. The results showed an agreement between model prediction and experimental observation. Since other factors may influence the permeate flux, more experiments should be done in order to optimize and validate this model for its application in a wider area of process conditions and tested suspensions.

Acknowledgements. The Grant Agency of the Czech Republic, Grant Project No. 104/00/0794, provided the financial support.

SYMBOLS

J	permeate flux	m s^{-1} (dm^3 m^{-2} h^{-1})
J_0	pure water permeate flux	m s^{-1} (dm^3 m^{-2} h^{-1})
J_{S}	steady-state permeate flux without intensification	m s^{-1} (dm^3 m^{-2} h^{-1})
$J_{\mathrm{S\,int.}}$	steady-state permeate flux with intensification	m s^{-1} (dm^3 m^{-2} h^{-1})
k	gas flow velocity factor, eqn (*8*)	
ΔP	transmembrane pressure difference	Pa
r	injecting ratio, eqn (*9*)	
R	resistance	m^{-1}
R'	specific resistance	m^{-2}
t	time	s
u'_{L}	superficial liquid flow velocity	m s^{-1}

u'_{G}	superficial gas flow velocity	m s^{-1}
w_{F}	mass fraction of dispersion in the feed	
δ_{C}	cake thickness	m
μ_0	permeate viscosity	Pa s
Φ_{C}	maximum solid volume fraction in the cake	
Φ_{F}	solid volume fraction in the feed	

REFERENCES

1. Mikulášek, P., *Collect. Czech. Chem. Commun. 59*, 737 (1994).
2. Cui, Z. F. and Wright, K. I. T., *J. Membr. Sci. 117*, 109 (1996).
3. Cui, Z. F., Bellara, S. R., and Homewood, P., *J. Membr. Sci. 128*, 83 (1997).
4. Li, Q. Y., Cui, Z. F., and Pepper, D. S., *Chem. Eng. J. 67*, 71 (1997).
5. Mercier, M., Fonade, C., and Lafforgue-Delorme, C., *Biotechnol. Tech. 12*, 853 (1995).
6. Mercier, M., Fonade, C., and Lafforgue-Delorme, C., *J. Membr. Sci. 128*, 103 (1997).
7. Cabassud, C., Laborie, S., and Lainé, J. M., *J. Membr. Sci. 128*, 93 (1997).
8. Laborie, S., Cabassud, C., Durand-Bourlier, L., and Lainé, J. M., *Filtr. Sep. 34*, 887 (1997).
9. Lee, Ch. K., Chang, W. G., and Ju, Y. H., *Biotechnol. Bioeng. 41*, 525 (1993).
10. Vera, L., Delgado, S., and Elmaleh, S., *Chem. Eng. Sci. 55*, 3419 (2000).
11. Ghosh, R. and Cui, Z. F., *J. Membr. Sci. 162*, 91 (1999).
12. Cakl, J., Bauer, I., Doleček, P., and Mikulášek, P., *Desalination 127*, 189 (2000).
13. Davis, R. H., *Sep. Purif. Methods 21*, 75 (1992).
14. Mikulášek, P. and Pospíšil, P., *Sci. Pap. Univ. Pardubice, Ser. A 6*, 79 (2000).
15. Pospíšil, P., *Diploma Thesis*. Department of Chemical Engineering, University of Pardubice, 1999.
16. Mikulášek, P. and Doleček, P., *Sep. Sci. Technol. 29*, 1183 (1994).
17. Laborie, S., Cabassud, C., Durand-Bourlier, L., and Lainé, J. M., *Chem. Eng. Sci. 54*, 5723 (1999).